Exploring Role of Accessory Pathway Location in Wolff-Parkinson-White Syndrome in a Model of Whole Heart Electrophysiology

Karli Gillette [1,2], Matthias AF Gsell [1], Stefan Kurath-Koller [3], Martin Manninger [4], Anton J. Prassl [1,2], Daniel Scherr [4], Gernot Plank [1,2]

[1] Gottfried Schatz Research Center : Biophysics, Medical University of Graz, Graz, Austria
[2] BioTechMed-Graz, Graz, Austria
[3] Division of Pediatric Cardiology, Department of Pediatrics, Medical University of Graz, Graz, Austria [4] Division of Cardiology, Department of Medicine, Medical University of Graz, Graz, Austria

Abstract

Introduction: *The location of the accessory pathway (AP) in Wolff-Parkinson-White (WPW) may serve as a bio-marker for patient morbidity. We therefore aimed to investigate the influence of the location of a typical AV bypass tract on the 12 lead ECG using a physiologically-detailed whole heart model of electrophysiology (EP) that is capable of providing in-depth information on the underlying electrical mechanisms of WPW.*

Methods: *In previous work, a physiologically-detailed model of whole heart EP was built and personalized for a single subject to generate a realistic normal sinus rhythm. Locations of APs used were automatically inserted within the heart using universal ventricular coordinates (UVCs) to model a typical AV bypass tract. For every location, cardiac sources and 12 lead ECGs were computed using an efficient cardiac simulator. 12 lead ECGs were evaluated for clinical markers of WPW. Electrical mechanisms are explored for two locations exhibiting highest and lowest morphological differences in the 12 lead ECG.*

Results: *Retrograde activation of the His-Purkinje System (HPS) that later merges with the wave-front stemming from normal activation of the HPS is observed. Not all APs resulted in 12 lead ECGs exhibiting morphological markers for WPW under clinical evaluation. This may be due to the representation of the AP or inherent dynamics of WPW.*

1. Introduction

WPW syndrome is a common clinical disorder affecting up to 2.0% of the population leading to paroxysmal palpitations and morbidity through supraventricular tachycardias or sudden cardiac arrest [1]. The disease is classified by the presence of one or more APs allowing abnormal antegrade AV conduction outside of the normal conduction system through the AV node that connects with the His-Bundle of the ventricular HPS [2]. Although non-invasive localization of the AP using the 12 lead ECG or invasive electro-anatomical mapping has limitations, the location of the AP may also serve as a bio-marker for the extent of disease manifestation and morbidity, as well as ablation success [3].

Clinical studies have therefore been conducted to explore the influence of location of APs on clinically relevant ECG metrics in the 12 lead ECG indicative of cardiac disease and the prognosis of patients [4]. Clinical studies are limited, however, due to ethical and experimental limitations and fail to offer insight into electrical phenomena. *In silico* cardiac models of EP have been utilized to both understand the actual mechanisms of WPW within the heart and to assist in automated localization approaches. However, previous *in silico* studies have only been performed on simplified models due to computational restrictions.

We therefore aimed to investigate the underlying electrical mechanisms of WPW with a typical short AV bypass tract allowing antegrade conduction from the atria to the ventricles. To explore the role of location on the 12 lead ECG, locations of APs were automatically sampled within the electrically-isolated basal surface using UVCs. Simulated 12 lead ECGs are compared to healthy sinus rhythm and evaluated using clinical markers. For two locations producing the minimal and maximal morphological variation in the 12 lead ECG, electrical phenomena within the heart are detailed.

2. Methods

Within previous work, a model of ventricular EP was built from clinical magnetic resonance images and personalized according to clinically-recorded 12 lead ECGs for a single subject (male, 45 years of age) [5]. This model was extended to include a more physiologically-detailed representation of the HPS [6]. Atrial EP was then accounted for

and delayed AV conduction was allowed through an AV node located at the base of the right atrium connected to the HPS. Both ventricular outflow tracts were assigned as generic tissue in the torso volume conductor. Repolarization was dictated by gradients in action potential duration within the Mitchell-Schaeffer ionic model that were implemented by assuming a linear relationship with activation as reported within experimental work [7–9]. To automatically control and alter parameters of EP, the model had been equipped with an abstract reference frame comprising both UVCs [10] and universal atrial coordinates [11]. For full details and intricacies on the model and personalization, we refer to [5, 6, 8].

2.1. Sampling Schematic

Locations of APs allowing antegrade conduction within the electrically-isolated basal surface of the heart were automatically sampled using UVCs [5]. Within each ventricles, the rotational coordinate was sampled 20 times through the full rotational range. Within the left and right ventricles, the rotational limits are $\pm\pi$ and $\pm\pi/2$, respectively. For each rotational value, an AP was then sampled at the endocardium ($\rho = 0$). As the ventricular outflow tracts were not considered conductive myocardium, locations within this region were removed from the sampling set. In total, 16 left-sided and 7 right-sided locations were sampled to total 23 APs.

2.2. Cardiac Simulation

Only a single heart beat wass modeled. Underlying cardiac sources and the 12 lead ECGs were computed for every sampled AP location in addition to normal sinus rhythm. Cardiac activation and repolarization was simulated using the reaction-Eikonal method in the monodomain formulation without diffusion [12]. 12 lead ECGs were computed using lead field matrices [13]. The simulation framework was implemented within *CARPentry* [14] and the *openCARP* simulation environment [15].

2.3. ECG Analysis

All 12 lead ECGs were filtered using a low-pass $60\,\mathrm{Hz}$ filter in accordance with typical clinical filter settings. To account for amplitude scaling occurring in lead field projection, all signals were also scaled by 0.275. The extent of morphological variation from the 12 lead ECG under normal sinus rhythm was quantified using a L2-norm.

3. Results

UVCs could be used to automatically sample locations of APs within the electrical isolation layer of the ventricles. Highest and lowest observed losses of 0.82 and 0.45 occur in locations on the anterior side of the left ventricular near the right ventricular outflow tract and on the endocardium of the right-ventricular free wall, respectively (both indicated on Fig. 1A). Not all 12 lead ECGs exhibit features indicative of WPW. Within sites located on the right-ventricular free wall and for a site located on the posterior left-ventricular free wall normal sinus rhythm is mostly maintained.

At the location on the right-ventricular free wall, normal sinus rhythm is mostly maintained as the pre-excitation of the right ventricle progresses slowly and does not disrupt normal activation of the left ventricle (bottom panel Fig. 2). A merging of the two wave-fronts is observed and results in activation resembling normal sinus rhythm (compare $275\,\mathrm{ms}$ on bottom and top panels in Fig. 2). Although a delta wave is more present than under sinus conditions, a prolonged PR interval outside clinical markers for WPW is thus observed from this activation pattern. The expected negative deflection in V1 is however, observed due to a lack of left-ventricular activation and a right-ventricular wave-front that generates no positive signal for V1.

When the location of the AP is located on the anterior-side of the left-ventricular epicardium, as seen in the highest loss, activation of the ventricles occurs altogether earlier but in a similar pattern (center panel in Fig. 2). All common markers of WPW include a shortened PR interval, presence of a delta wave, and a QRS complex greater than $120\,\mathrm{ms}$ were observed within the 12 lead ECG in this location. Note that precordial leads V1 and V2 have a strong positive deflection resulting from more basal activation of the right ventricle from the left-ventricular septum (see $200\,\mathrm{ms}$ and $225\,\mathrm{ms}$ in center panel of Fig. 2) agreeing with clinical markers for Type A WPW. Earlier onset or inversion of the T-wave is observed as abnormal repolarization is linked to abnormal activation.

4. Discussion

Mechanisms underlying WPW were studied within a personalized and physiologically-detailed model of whole heart EP of a single subject. Locations of APs allowing antegrade conduction were sampled within the electrically-isolated basal surface and simulated using an efficient cardiac simulator. Data developed during this study could be used for localization algorithms when expanded to a larger model cohort capable of representing the WPW patient population.

A more complex model of the AV bypass tract is needed, as simulated 12 lead ECGs for sampled locations of APs (Figure 1A) did not consistently exhibit standard clinical manifestations of WPW for the relevant type (Fig. 1B). Pathways are known to behave more similar to a Purkinje fiber of various lengths stemming from an atrial insertion

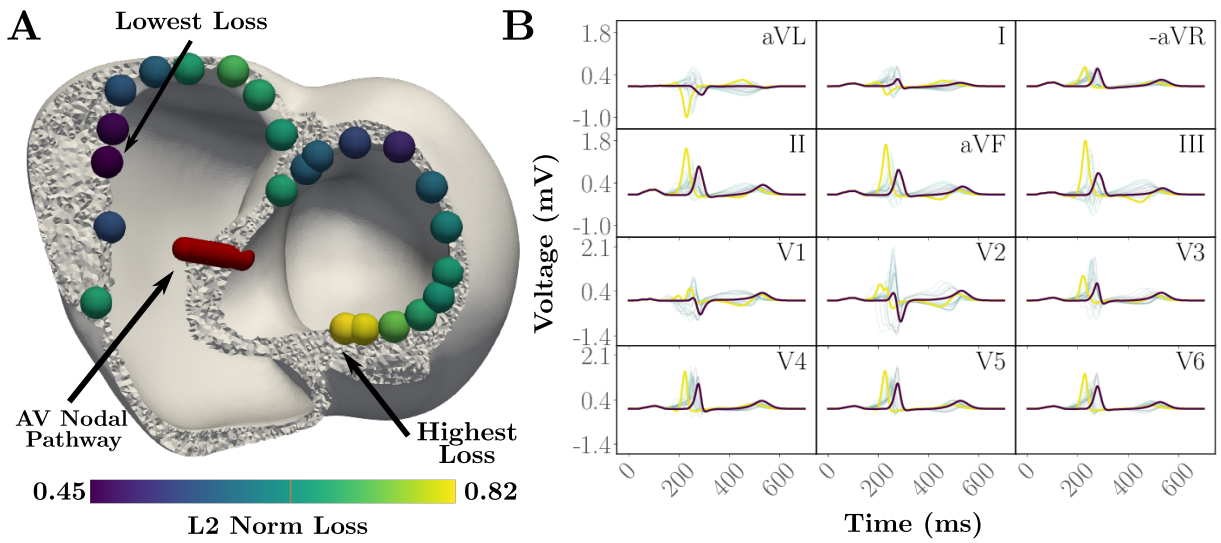

Figure 1. Locations of APs within the electrically-isolated basal surface (**A**) lead to morphological variations in the 12 lead ECG (**B**). Coloration corresponds to the L2-norm compared to the simulated 12 lead ECG under normal sinus rhythm (black). The locations with the highest and lowest observed L2-norms are indicated. Location of the AV nodal pathway is also indicated and colored in red.

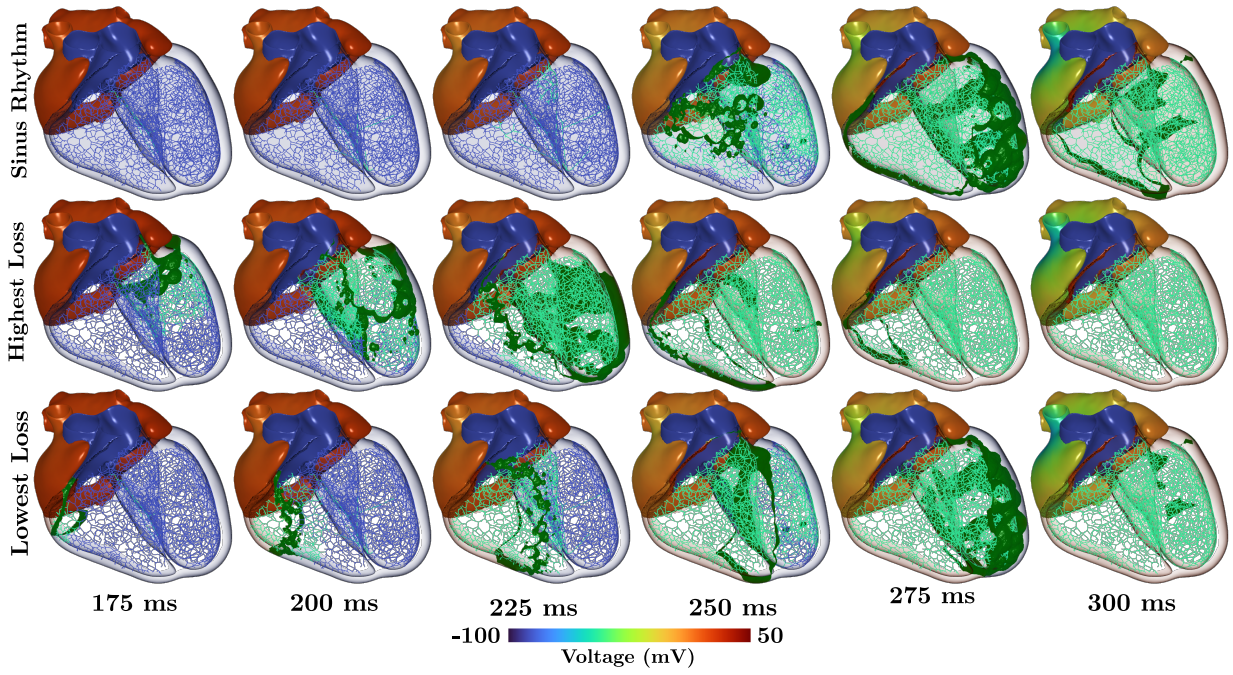

Figure 2. Trans-membrane voltage within the heart for a single AP resulting in the highest (center) and lowest (bottom) morphological differences in the 12 lead ECG in contrast to normal sinus rhythm (top). Membrane voltages for the atria are color-coded according to the color map. Green isolines in the ventricles indicate $-40\,\mathrm{mV}$.

point to the ventricles. This facilitates shortened PR intervals and the onset of the delta wave. Different conduction properties of both the HPS and the AP could then be explored. The existence of APs within the the right and left-ventricular outflow tracts should also be considered.

Various other types and mechanisms of WPW must be modeled to gain clinical viability in later studies. Namely, the most frequent arrhythmia in WPW termed orthodromic

AV re-entrant tachycardia, characterized by antegrade conduction of the HPS and retrograde conduction over the AP, was not yet modeled due to limitations in the simulation framework. Modelling during pacing near the AP or during atrial fibrillation instead of normal sinus rhythm may reveal more clear signs of pre-excitation that could be compared to standard diagnostic algorithms. Mechanisms leading to sudden cardiac death and ventricular tachycardia within WPW were also not yet explored and remain unclear. Regardless, the model presented is a first step towards understanding more complex pathways *in silico*.

Acknowledgments

This research was supported by funds received from BioTechMed-Graz under the ILearnHeart Flagship Project and under grant I2760-B30 from the Austrian Science Fund to GP. This project conducted under MedalCare 18HLT07 has received funding from the EMPIR programme co-financed by the Participating States and from the European Union's Horizon 2020 research and innovation programme. This research has also received funding from the European Union's Horizon 2020 research and innovation programme under the ERA-NET co-fund action No. 680969 (ERA-CVD SICVALVES) funded by the Austrian Science Fund (FWF), Grant I 4652-B to CMA.

References

[1] Lu CW, Wu MH, Chen HC, Kao FY, Huang SK. Epidemiological profile of wolff–parkinson–white syndrome in a general population younger than 50 years of age in an era of radiofrequency catheter ablation. International journal of cardiology 2014;174(3):530–534.

[2] Issa Z, Miller JM, Zipes DP. Clinical Arrhythmology and Electrophysiology: A Companion to Braunwald's Heart Disease E-Book: Expert Consult: Online and Print. Elsevier Health Sciences, 2012.

[3] Ardakani MB, Dehghani F, Sarebanhassanabadi M, Yalameh A, Behjat M, Ardakani MB, Shafiee M, Hosseini SMS. Impact of accessory pathway location on electrophysiologic characteristics and ablation success. Critical Pathways in Cardiology 2020;19(2):94–97.

[4] de Chillou C, Maria Rodriguez L, Schläpfer J, Kappos KG, Katsivas A, Baiyan X, Smeets JL, Wellens HJ. Clinical characteristics and electrophysiologic properties of atrioventricular accessory pathways: importance of the accessory pathway location. Journal of the American College of Cardiology 1992;20(3):666–671.

[5] Gillette K, Gsell MA, Prassl AJ, Karabelas E, Reiter U, Reiter G, Grandits T, Payer C, Štern D, Urschler M, et al. A framework for the generation of digital twins of cardiac electrophysiology from clinical 12-leads ecgs. Medical Image Analysis 2021;71:102080.

[6] Gillette K, Gsell MA, Bouyssier J, Prassl AJ, Neic A, Vigmond EJ, Plank G. Automated framework for the inclusion of a his–purkinje system in cardiac digital twins of ventricular electrophysiology. Annals of biomedical engineering 2021;49(12):3143–3153.

[7] Opthof T, Coronel R, Janse MJ. Is there a significant transmural gradient in repolarization time in the intact heart? repolarization gradients in the intact heart. Circulation Arrhythmia and Electrophysiology 2009;2(1):89–96.

[8] Gillette K, Gsell MAF, Strocchi M, Grandits T, Neic A, Manninger M, Scherr D, Roney CH, Prassl AJ, Augustin CM, Vigmond EJ, Plank G. A personalized real-time virtual model of whole heart electrophysiology. Frontiers in Physiology 2022;13. ISSN 1664-042X.

[9] Mitchell CC, Schaeffer DG. A two-current model for the dynamics of cardiac membrane. Bulletin of mathematical biology 2003;65(5):767–793.

[10] Bayer JD, Blake RC, Plank G, Trayanova NA. A novel rule-based algorithm for assigning myocardial fiber orientation to computational heart models. Annals of biomedical engineering 2012;40(10):2243–2254.

[11] Roney CH, Pashaei A, Meo M, Dubois R, Boyle PM, Trayanova NA, Cochet H, Niederer SA, Vigmond EJ. Universal atrial coordinates applied to visualisation, registration and construction of patient specific meshes. Medical image analysis 2019;55:65–75.

[12] Neic A, Campos FO, Prassl AJ, Niederer SA, Bishop MJ, Vigmond EJ, Plank G. Efficient computation of electrograms and ecgs in human whole heart simulations using a reaction-eikonal model. Journal of computational physics October 2017;346:191–211. ISSN 0021-9991.

[13] Potse M. Scalable and accurate ecg simulation for reaction-diffusion models of the human heart. Frontiers in physiology 2018;9:370.

[14] Vigmond E, Dos Santos RW, Prassl A, Deo M, Plank G. Solvers for the cardiac bidomain equations. Progress in biophysics and molecular biology 2008;96(1-3):3–18.

[15] Plank G, Loewe A, Neic A, Augustin C, Huang YL, Gsell MA, Karabelas E, Nothstein M, Prassl AJ, Sánchez J, et al. The opencarp simulation environment for cardiac electrophysiology. Computer Methods and Programs in Biomedicine 2021;208:106223.

Address for correspondence:

Karli Gillette
Neue Stiftingtalstraße 6/D04, A-8010 Graz, Austria
karli.gillette@medunigraz.at